EFFICIENT SIMULATION OF A TWO-PHASE VERTICAL PIPE FLOW WITH POPULATION BALANCE METHOD

Matteo ICARDI[12*], Daniele L. MARCHISIO[2] and Mathieu LABOIS[3]

[1] DIATI, Politecnico di Torino, Corso Duca degli Abruzzi 24, 10129 Torino, ITALY

[2] DISAT, Politecnico di Torino, Corso Duca degli Abruzzi 24, 10129 Torino, ITALY

[3] Ascomp GmbH, Technoparkstrasse 1, Zurich, SWITZERLAND

*Corresponding author, E-mail address: matteo.icardi@polito.it

ABSTRACT

The population balance equation for bubble size distribution in a vertical turbulent pipe flow is solved with a Direct Quadrature Method of Moment (DQMOM) comparing the results with a classical approach where bubbles are characterized by their mean size. The turbulent two-phase flow field, solved within a RANS formulation, is assumed to be in local equilibrium and the relative gas and liquid velocities are therefore calculated with an algebraic slip model, considering drag and lift forces. The non-linear relation between the bubble size and the resulting forces is accurately described through the DQMOM method, in which each quadrature node represents a dynamic class of particles with a characteristic size. Results are compared to experimental results (Szalinski et al., 2010), demonstrating that fast and accurate predictions are obtained for the void fraction and the bubble size distribution in the case of moderate bubble Stokes number and void fraction.

NOMENCLATURE

L liquid (subscript)
G gas (subscript)
d bubble diameter
p pressure
n bubble size distribution (number per unit volume)
V^m mixture velocity
V^S slip/relative velocity
V^d drift/diffusion velocity
ρ density
α gas volume fraction
μ dynamic viscosity
Y mass fraction

INTRODUCTION

Nowadays in many important industrial fields (in particular in the petroleum and chemical industry) there is a urgent need of mathematical models and numerical framework characterized by a good accuracy and predictivity coupled with low computational costs. This is true in particular for turbulent multiphase flows like bubble columns or pipe flows where a liquid and a gas phase are present and fully resolved approaches (e.g., explicit interface reconstruction) are not viable. The objective of this work is to test and validate a fast Eulerian-Eulerian method to solve gas-liquid flow based on the Algebraic Slip Model (ASM) and the Direct Quadrature Method of Moments (DQMOM).

The test case under study is a two-phase flow of gas and water across a vertical tube of 0.067 m diameter and has been experimentally investigated by Szalinsky et al. (2010). The height of the tube is 6 m. Superficial velocities of air and water are given as inflow boundary conditions, and the average gas concentration is measured at a height of 5 m.

The liquid superficial velocity is below 1.0 m/s and the gas superficial velocity below 0.1 m/s. This leads to a flow regime predominated by pure bubbly flow (with spherical or cap shape). The two inflow velocities investigated are represented with red symbols on the flow pattern map in Figure 1, characterized by superficial liquid velocity of 0.2 and 0.7 m/s and a constant superficial gas velocity of 0.05 m/s. The Reynolds numbers, based on the mixture properties at the inflow and the tube diameter is respectively of 17000 and 47000.

Inflow conditions are set by giving superficial velocities of gas and water. Because no other data are available for the inflow boundary conditions, it is therefore assumed that the velocity and void fraction profiles are flat and the average void fraction is extrapolated from experimental data. Pressure outflow boundary condition is used at the exit of the tube.
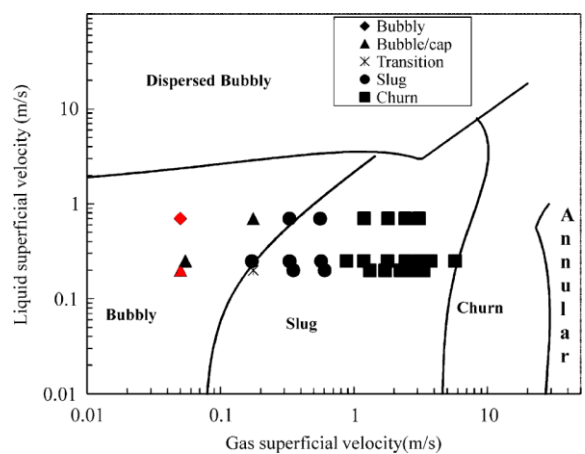
Figure 1: Gas-liquid flow regimes (Szalinsky et al., 2010). Red symbols indicate the cases investigated in this work, corresponding to the bubbly flow regime.

MODEL DESCRIPTION

Multiphase flow model

Incompressible Navier-Stokes methods are assumed to hold for each phase. A mixture model, in which a single momentum equation is solved for the mixture velocity, is used, with algebraic relation to solve slip velocities. This model can be written as follows:

$$\frac{\partial \rho^m}{\partial t} + \frac{\partial}{\partial x_j}\left(\rho^m V_j^m\right) = 0 \tag{1}$$

$$\rho_G \frac{\partial \alpha_G}{\partial t} + \rho_G \frac{\partial}{\partial x_j}\left(\alpha_G(V_j^m + V_{G_j}^d)\right) = 0 \tag{2}$$

$$\frac{\partial \rho^m V_i^m}{\partial t} + \frac{\partial}{\partial x_i}\left(\rho^m V_i^m V_j^m + \rho^m \frac{Y_G}{Y_L}V_{G_i}^d V_{G_j}^d\right) = -\frac{\partial p^m}{\partial x_i}$$
$$+ \frac{\partial}{\partial x_j}(2\mu^m S_{ij}^m) + \frac{\partial}{\partial x_j}(2\alpha_G \mu_G S_{G_{ij}}^d) + \frac{\partial}{\partial x_j}(2\alpha_L \mu_L S_{L_{ij}}^d) \tag{3}$$

where the subscripts G and L denote respectively the gas and liquid phase and the phase interaction term S_L^d is

$$S_{L_{ij}}^d = -\frac{1}{2}\left[\frac{\partial}{\partial x_j}\left(\frac{Y_G}{Y_L}V_{G_i}^d\right) + \frac{\partial}{\partial x_i}\left(\frac{Y_G}{Y_L}V_{G_j}^d\right)\right] \tag{4}$$

The above equations are written in the assumption of gas and liquid incompressibility that is valid for low void fraction and constant temperature. The drift velocities of gas and liquid are calculated with the Algebraic Slip Model (ASM) in the formulation of Manninen et al. (1997). They can be found from the force balance

$$F_D + F_L = -\frac{\rho_G - \rho^m}{\rho^m}\nabla p \tag{5}$$

where for this test case only drag and lift forces are considered and expressed in terms of slip (or relative) velocities as

$$F_D = \frac{3}{4}C_D\frac{\rho_L}{d}|V^s|V^s \tag{6}$$

$$F_L = C_L\rho_L V^s \times \nabla \times V_L \tag{7}$$

where C_D and C_L are given by the Tomiyama correlation (Tomiyama, 1998). The relation between drift and slip velocities is then given by

$$V_i^d = V_i^s - \sum_i Y_i V_i^s, \quad i = G, L \tag{8}$$

The turbulence is taken into account introducing a turbulent dispersion for bubbles, modifying the drift velocities as follows:

$$V^d = V_0^d + (1 - Y_G)\frac{\mu_T}{\rho^m}\nabla\alpha_G \tag{9}$$

Population balance model

The model described above need the bubble size as an input parameter for the drag and lift coefficients. This is however an evolving heterogeneous quantity because of bubble coalescence and breakup. Furthermore in the same computational (or averaging) volume a wide range of bubble diameters can coexist. To describe more

accurately the evolution of the bubbles in the riser, instead of solving an equation for the gas volume fraction, a population balance equation (PBE) can be introduced. This equation describes the evolution in time and space of the bubble size distribution (BSD) $n(d;\boldsymbol{x},t)$ that represents the number of bubbles per unit volume with size d and can be written as

$$\frac{\partial}{\partial t}n + \frac{\partial}{\partial x_j}V_{p_j}(d)n + \frac{\partial}{\partial d}Gn = C(n,n) + B(n) \tag{10}$$

where V_p is the velocity of the dispersed phase (which in this case is given by the algebraic slip model), G is the growth term (null if there is no phase change or mass transfer) and B and C are the collision terms describing respectively bubble coalescence (that is a two-point process and has a double dependence on the distribution) and breakup (that is a one-point process with a single dependence on the distribution). In this work these phenomena are described with the kernel used by Laakkonen et al. (2006).

All the equations are solved within a Reynolds average formulation and the k-ε model has been used to model Reynolds stresses. The averaging procedure applied to Eq. 10 gives place to a turbulent fluctuation term, modelled with a turbulent diffusivity term with a constant $D_t = v_t\,Sc_t$ and a turbulent Schmidt number $Sc_t = 0.9$.

The population balance equation is discretized with the Direct Quadrature Method of Moments (DQMOM, Marchisio and Fox, 2005) which consists in the resolution of transport equations for quadrature nodes and weights that approximates exactly the first M moments of the BSD. Each node, corresponding to a particular bubble size, and its corresponding weight are transported with their relative velocity (calculated with the ASM) and can be considered as a dynamic class with a certain size and a weight that represents the number of bubbles per unit volume within that class. This results in higher accuracy and lower computational cost than the standard classes methods. In the test case under study it has been demonstrated that accurate results are already obtained with $M=4$, tracking exactly (except numerical discretization errors) moments up to third order.
It is important to underline that, when the population balance is solved there is no need to solve the equation for the total gas volume fraction but this is obtained implicitly as a multiple of the third order moment of the BSD. Therefore the simulation require to solve only 3 scalar equations more than the classic ASM model.

NUMERICAL METHODS

The models described above have been implemented in commercial CFD code TransAT. The different modelling possibilities to describe this type of multiphase flows are shown in Table 1. In addition to these models a population balance, solved with the DQMOM approach can be coupled to describe the dispersed phase.

With the objective of simplify the simulation to later extent this model to more complex pipe systems, we decided to use a RANS k-ε model and to assume a two-

dimensional axisymmetric domain giving place to a steady-state solution.

Homogeneous model with algebraic slip model				
3D simulation			2D axisymmetric simulation	
V-LES	k-ε model		k-ε model	
Unsteady	Unsteady	Steady	Unsteady	Steady

Table 1: Modelling approaches for turbulent two-phase flows (Ascomp, 2012)

The steady-state solution can be obtained either by directly employing a steady-state iteration or through marching in time until steady-state conditions are reached. To consider the effects of large-scale fluctuations also unsteady simulations, with the Very-Large Eddy Simulation (V-LES) method, has been tested. This method is based on the concept of filtering a larger part of turbulent fluctuations as compared to LES. The V-LES used in TransAT is based on the use of the k-ε model as a sub-filter model. A filter is applied to this model, so that turbulent structures smaller than the filter width are not solved. A length-scale limiting function f has been derived in Johansen (2004) and can be written as

$$f\left(C_3\Delta\frac{\varepsilon}{k^{3/2}}\right) = \mathrm{Min}\left(1, C_3\Delta\frac{\varepsilon}{k^{3/2}}\right) \quad (11)$$

where Δ is the filter width and

$$C_3 = \frac{\gamma}{4C_\mu\sqrt{3/2}} = 1.0 \quad (12)$$

is a constant and γ is the anisotropic factor. Applying this function to the k-ε model gives the following expression for turbulent viscosity

$$\nu_t = C_\mu\mathrm{Min}\left[1, C_3\Delta\frac{\varepsilon}{k^{3/2}}\right]\frac{k^2}{\varepsilon} \quad (13)$$

Near the wall boundaries, the length-scale limiting function is set equal to one, which means that the standard k-ε model is applied. This enables one to use standard wall-function of RANS models for V-LES.

SIMULATION DETAILS

The spatial derivatives have been discretized with the HLPA scheme (Zhu, 1991) which is in this case the best compromise between accuracy and stability. Since the drag and lift forces used are highly non-linear, a small diffusivity is added to the solution to stabilize the evolution of the flow in the first part of the riser near the wall where the most dramatic changes happen.

The equations for nodes and weights are characterized by having locally large source terms because of the collision kernel. Even if an implicit solver (SIP solver) has been used, a fully implicit treatment of the source terms is not possible because of the high non-linearity. Therefore a sophisticated source term linearization and relaxation has been implemented to stabilize the computations. First the coupled system of equations for nodes and weights is relaxed with the maximum eigenvalue of the system, then a special treatment to avoid critical values for DQMOM

variables is performed. In fact, although the DQMOM formulation (where weights and weighted nodes are transported) presents many advantages with respect to the original QMOM formulation (where moments are transported), it can blows up when dealing with mono-disperse populations or equivalently when the distance between two quadrature nodes approaches zero. This problem can be solved either with an adaptive DQMOM (reducing locally the number of quadrature nodes and weights) or preventing the systems to reach these critical states during the internal sub-iterations or time steps. This second solution is the one adopted in this work, where we can suppose that the real solution is never mono-dispersed. It is important to highlight that this source term treatment is only a numerical trick to enhance convergence and stability while it is not affecting the consistency of the model (i.e., the system converge to the exact numerical solution in the limit of null residuals). DQMOM has been solved with $M=4$ and $M=6$ resulting in very similar results therefore in the following results only the case with $M=4$ is shown.

Simulations have been performed on a single core of a Intel XEON X5690. 2D steady simulations with k-ε model have taken less than one hour of CPU time to converge to a maximum normalized residual of 10^{-5} on a mesh of 507x24 cells (tube of 5.0 m). Also 3D unsteady simulations with the V-LES model have been performed to understand if large scale fluctuations could be present affecting the overall results. Indeed, although the flow under survey is unsteady, it reaches a well-defined steady state (in a time-averaged sense). If results are not sensitive to the fact that we use steady or unsteady simulations, then a lot of computational time can be saved.

It resulted that steady and unsteady void fraction profiles, reported in Figure 2 are very close to each other in terms of gas volume fraction profiles. This is in agreement with the fact that the flow reaches a statistical steady state where large scale fluctuations are not important. Therefore, in the current study, only 2D axisymmetric results with k-ε model will be presented, because obtained results are acceptable and 3D unsteady simulations are significantly more expensive in terms of computational cost. A more detailed analysis of 3D unsteady simulations will be considered for further investigations especially when more complex geometries will be taken into account. In fact, asymmetric and complex geometries can affect the turbulent flow field with strong anisotropy and more complex flow structures that are better resolved with unsteady simulations.

A set of simulations have been then performed in order to define which size of the domain is needed, and what is the required refinement in order to obtain a grid independence of the results. This analysis, as well as the following results, has been performed using a 2D axisymmetric and steady simulations.
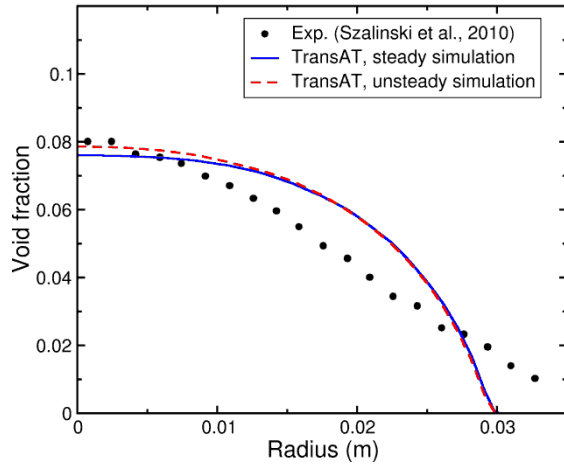
Figure 2: Comparison of void fraction profiles for steady and unsteady simulation

A first study has been performed on the size of the grid cells (Figure 3). Simulations have been performed on a tube of 5.1m long, with a coarser mesh of 307 x 15 cells (Δx=0.016 m, Δy_{min}=0.001 m) and a finer mesh consisting in 507 x 24 cells (Δx=0.01 m, Δy_{min}=0.0004 m). No further refinement have been performed, because since y^+=11 on the fine mesh, and further refinement would mean changing the near-wall treatment of turbulence. Void fraction and velocity profile were analyzed and resulted quite close one to each other at the centre of the tube, which means that grid independence is almost reached. However, there is an important loss of precision with the coarser mesh close to the wall. Therefore only the results on the mesh of 507 x 24 will be presented.
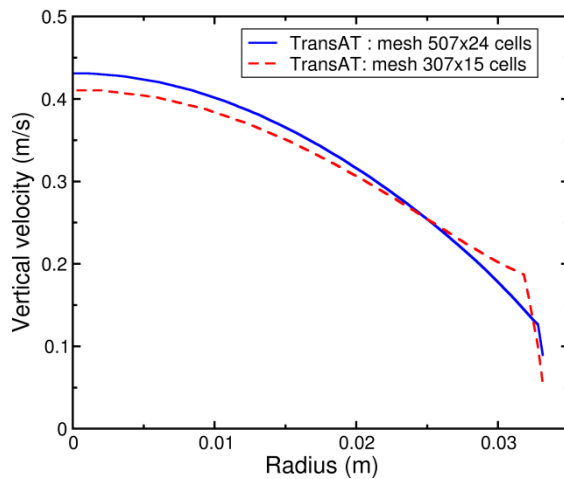
Figure 3: Grid convergence study. Velocity profiles at height *x*=5 m for two mesh refinements.
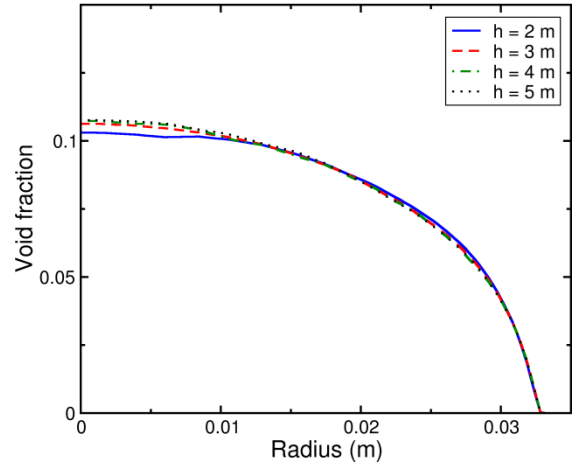
Figure 4: Domain height study. Void fraction profiles in different sections at height 2,3,4,5 m.

A second analysis has been performed on the length of the tube (Figure 4). Indeed, simulating the full domain can be costly, whereas it is only needed to have a fully developed flow to measure the void fraction distribution, which will not change once the flow is fully developed. Experiments suggest that the flow is developed after 3 m. Simulations have then been performed on a 5.1 m long tube, and profiles of the void fraction at different heights demonstrated that simulating 3 m is enough (equivalent to a length-to-diameter ration of L/D=44.7).

RESULTS

The main case studied consists in a liquid superficial velocity of 0.2 m/s and a gas superficial velocity of 0.05 m/s. In the experiments, bubbles are released from holes of diameter 3 mm but merging happens immediately in the vicinity of the sparger. The Tomiyama's model which has been used to model lift force, changes its behaviour for a radius of 2.9 mm. Thus, in the simulation with the standard ASM (fixed bubble radius without PBE model) the bubble radius has been fixed to 2.92 mm, which gives a bubble Reynolds number Re_b=2450. Instead the simulations performed with the population balance models are performed with an inlet BSD equivalent to a log-normal distribution with mean value 5.8 mm and a standard deviation of 1.5 mm. This distribution was estimated with the procedure explained in Petitti et al. (2010).
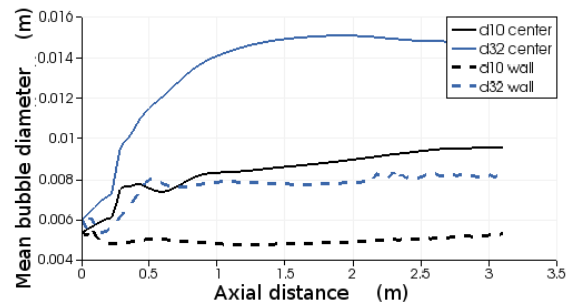
Figure 5: Evolution of the mean bubble diameter along the riser near the wall and in the center of the pipe.

In Figure 5 the evolution of the mean bubble diameter along the pipe is shown for a position near the wall and in the center of the pipe. The mean diameter is calculated as the first moment of the BSD divided by the total number of bubbles (d10) or as the ratio between the third and the second order moments (d32). The difference between these estimations of the mean bubble size is also a quantification of the poly-dispersity of the distribution and on the importance of solving the population balance model without imposing a fixed mean size for the bubbles. Two concurrent phenomena are causing the formation of large bubbles in the center of the pipe and small bubbles near the wall. On one side this is due to the lift force correlation that depends on the bubble size. On the other side the coalescence and breakage events are highly influenced by the presence of the wall.
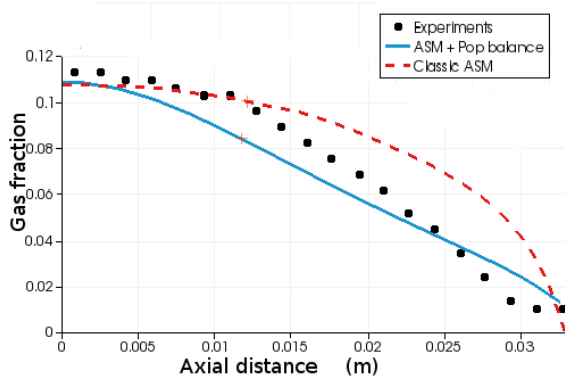
Figure 6: Gas volume fraction profile at the end of the riser. Experiments (symbols), classic ASM model (dashed line) and ASM with population balance model (continuous

As can be seen in Figure 6, where the gas volume fraction is shown for the ASM model with and without the population balance, simulation results are in good agreement with experimental data. The maximum void fraction, at the centre of the tube, is well predicted. The void fraction is slightly over predicted close to the wall for the classic ASM model without population balance, which may be due to the fact that the bubble coalescence is not simulated causing an underestimation of the lift force. When the population balance is solved the profile is closer to experiments and the remaining mismatch can be due to the inaccuracy of the lift and drag coefficients for large bubbles.
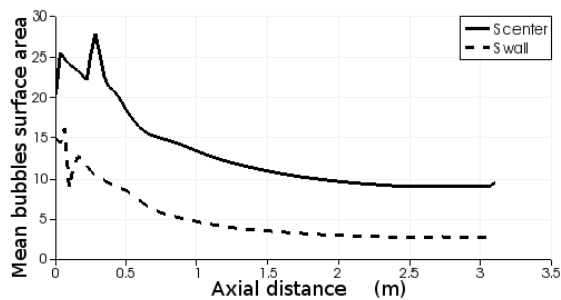
Figure 7: Evolution of the mean bubble surface area along the riser near the wall and in the center of the pipe.

The advantage of the population balance mode is that we can track a number of important physical quantities such as the bubble surface area that is a crucial quantity for

phase change, heat transfer and reaction. In Figures 7 and 8 respectively the mean bubble surface area (obtained as a multiple of the second order moment) and the number of bubbles per unit volume (equal the 0th order moment) is reported for the center of the pipe (continuous line) and a region near the wall.
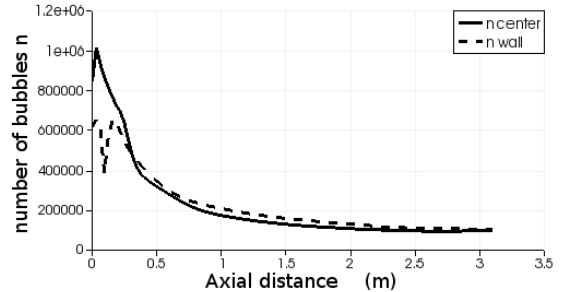
Figure 8: Evolution of the total number of bubbles per unit volume along the riser near the wall and in the center of the pipe.

The experimental results reported also the mean BSD at the end of the riser, revealing a bi-modal distribution with a first wide peak between 3 mm and 6 mm and the second one between 25 mm and 40 mm. This is consistent with our DQMOM results. Air and water velocity profiles can be also calculated from the simulations but no experimental data is available for comparison of the velocities. Since the superficial velocities are constant, it would be important in future analysis to be able to compare the velocities to experimental data to find out exactly the reasons for the differences in the void-fraction profiles.

Finally a flow with a liquid superficial velocity of 0.7 m/s and a gas superficial velocity of 0.05 m/s, which gives place to a Reynolds number of 47000 has been considered. In Figure 9 the gas volume fraction obtained with and without the population balance model is compared against experimental values. Also in this case the usage of the population balance model ensures a better approximation of the BSD in the pipe and this results also in a better approximation of gas velocity and therefore of volume fraction.
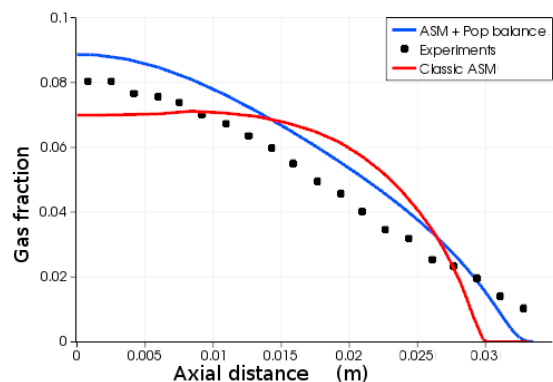
Figure 9: Gas volume fraction at the end of the riser for liquid superficial velocity equal to 0.7 m/s. Experiments (symbols), classic ASM model (dashed line) and ASM with population balance model (continuous line).

CONCLUSION

This work shows the capabilities of a computationally efficient algebraic mixture model coupled with a population balance model to predict dispersed bubbly and cap-bubbly flows in a vertical column. The simulation results obtained are in good agreement with the experiments performed by Szalinski et al. (2010) for the bubbly flow regime, although 2D axisymmetric conditions have been assumed in the simulations. It can also be safely concluded that the mixture model with algebraic slip model is appropriate for this kind of flow, provided that good empirical correlations are given for drag and lift forces, without using the two-fluid approach that is computational costly and can be affected by numerical instability. The present results can be easily extended to long piping systems thanks to the cheap computational setup and to more complex geometries with the use of an immersed boundaries technique implemented in the code.

The same model has been tested also for higher gas superficial velocities for which the formation of air slugs or Taylor bubbles are important. In this case it more complicated to model the flow because of the large structures and associated unsteady behaviour. Furthermore the algebraic slip model is well known to be well suited for the simulation of flows laden with small bubbles, of sizes comparable to the grid, and with moderate Stokes number. Furthermore the modelling of the drift velocity requires a well-defined bubble radius that is not available for slug flows. Also the population balance formulation in this case is not valid if the slugs predominates. For flows featuring large air scale structures, in fact, the phase average approach is not adequate. Therefore the model blows up giving inaccurate results . For these types of flow regimes an interface tracking model can be a better choice even if it would not solve the small air bubbles formed in the wake of the Taylor bubbles. Our future work will try to merge these two techniques and extend these results for more complex geometries with the use of the Immersed Surfaces Techniques (IST) available in the code.

REFERENCES

ASCOMP GmbH, (2012), "TransAT User Manual", http://www.ascomp.ch.

ICARDI, M.; MARCHISIO, D. L.; NARAYANAN, C. & FOX, R. O., (2012), "Equilibrium-Eulerian LES Model for Poly-disperse Particle-laden Channel Flow", *Int. J. Nonlinear Sci. Numer. Sim.,* submitted.

JOHANSEN, S. T.; WU, J. & SHYY, W., (2004), "Filtered-based unsteady RANS computations", *Int. J. Heat Fluid Flow, 25*, 10-21.

LAAKKONEN, M.; ALOPAEUS, V. & AITTAMAA, J., (2006), "Validation of bubble breakage, coalescence and mass transfer models for gas-liquid dispersion in agitated vessel, *Chem. Eng. Sci., 61*, 218-228.

MCGRAW, R., (1997), "Description of aerosol dynamics by the quadrature method of moments", *Aerosol Sci. Technol., 27*, 255-265.

MANNINEN, M. & TAIVASSALO, V., (1996), "On the mixture model for multiphase flow", VTT Publications.

MARCHISIO, D. L. & FOX, R. O., (2005), "Solution of population balance equations using the direct quadrature method of moments", *J. Aerosol Sci., 36*, 43-73.

PETITTI, M.; NASUTI, A.; MARCHISIO, D. L.; VANNI, M.; BALDI, G.; MANCINI, N. & PODENZANI, F., (2010), "Bubble Size Distribution Modeling in Stirred Gas-Liquid Reactors with QMOM Augmented by a New Correction Algorithm", *AIChE J., 56*, 36-53.

SZALINSKI, L.; ABDULKAREEM, L.; SILVA, M. D.; THIELE, S.; BEYER, M.; LUCAS, D.; PEREZ, V. H.; HAMPEL, U. & AZZOPARDI, B., (2010), "Comparative study of gas-oil and gas-water two-phase flow in a vertical pipe" *Chem. Eng. Sci., 65*, 3836-3848.

ZHU, J., (1991), "A low-diffusive and oscillation-free convection scheme", *Commun. Appl. Numer. Methods, 7*, 225-232.